Single frequency sound propagation in flat waveguides with locally reactive impedance boundaries

Hequn Min,[a] Weisong Chen, and Xiaojun Qiu
Key Laboratory of Modern Acoustics and Institute of Acoustics, Nanjing University, Nanjing, 210093, China

(Received 5 October 2010; revised 13 June 2011; accepted 16 June 2011)

A coherent image source method is presented for evaluating single frequency sound propagation from a point source in a flat waveguide with two infinite and parallel locally reactive boundaries. The method starts from formulating reflections of the spherical sound radiation into integrals of plane wave expansion, and the analytical evaluation of the integrals is simplified by introducing a physically plausible assumption that wave front shapes remain the same before and after each reflection on a reflective boundary. The proposed model can determine coherently the sound fields at arbitrary receiver locations in a flat waveguide, even when one boundary is highly sound absorptive. Being compared with the classical wave theory and the existing coherent ray-based methods, it is shown that the proposed method provides considerable accuracy and advantages to predict sound propagation in flat waveguides with a sound absorptive ceiling and a reflective floor over a broad frequency range, particularly at large distances from the source where the existing methods are problematic. © *2011 Acoustical Society of America*. [DOI: 10.1121/1.3608124]

PACS number(s): 43.50.Gf, 43.55.Ka, 43.55.Br [FCS] Pages: 772–782

I. INTRODUCTION

Speech privacy and noise control problems are often encountered in open-plan offices and appear serious when these rooms are large.[1] In such rooms, usually, lateral dimensions are much larger than the height, the ceiling is lined with sound absorptive material and the floor is reflective. A simplified model for such rooms can be a flat waveguide with two infinite and parallel boundaries (ceiling and floor) with locally reactive material.

The sound field inside a flat waveguide can be calculated by many methods. Kuttruff[2] proposed analytical formulas to predict the sound energy distribution in flat waveguides based on the incoherent image source method from the 1980s. Many other researchers have studied sound propagation in similar spaces, such as large fitted factories,[3–6] workshops,[7,8] and dining rooms.[9] These studies are either based on the incoherent image source methods or the ray-tracing techniques, which neglect the interference effect among the direct sound and the multiple reflections. However, it has been shown that the accuracy of prediction can be improved if a coherent model is used.[10] Further, in some applications, such as that for predicting sound fields of speech or narrow band noise, interference from different sound waves must be taken into account to provide meaningful prediction.[11,12]

There are some studies on the coherent ray-based prediction model for sound fields in bounded spaces. Dance *et al.*[10] have developed an interference model to predict the sound pressure in industrial enclosures by considering the sound propagating phase shift and coherent summation of different reflected waves. However, in their model, the inherent phase shift of sound waves before and after reflections on impedance boundaries are not taken into account and the incidence angle of each reflection was not properly considered. It is also found that the method cannot provide accurate results for receivers far away from the reflecting surfaces.[10] A few years later, Wang and Bradley[13] employed the image source method to calculate coherently the total field from a point source in open-plan offices by using the plane wave reflection coefficients for the successive reflections of spherical sound radiation of the point source. Unfortunately, little theoretical analysis was provided in their paper.

Brekhovskikh[14] described the sound field in a flat-layered homogeneous media as the sum of the direct sound and the multiple reflections from image sources, where each reflection is formulated as a plane wave expansion integral. Although the solution can be used in flat waveguides directly, large errors are observed in the circumstances with a sound absorptive ceiling and a reflective floor, especially at receivers far away from the source compared to the waveguide height (see Figs. 3 and 7 below), whereas such situation is often encountered in large open-plan offices.

In light of Brekhovskikh's work and based on the solution of the spherical wave reflection on an infinite plane, Gensane and Santon[15] proposed a generalized solution to effectively model successive reflections of spherical sound radiation from a point source in bounded spaces with several boundaries. The plane wave reflection form, which is just the first-order approximate solution of the spherical wave reflection on a plane, was adopted in their study to develop a complex image source method. The method was shown to be able to predict coherently the sound field in bounded spaces with sufficiently hard boundaries at high frequencies.[14,15]

According to the concepts of Gensane and Santon,[15] Lemire and Nicolas[11] replaced the reflection coefficient used in the method of Gensane and Santon with a more accurate solution[16] of the spherical wave reflection on an infinite plane to numerically investigate the sound field in flat waveguides. The method proposed by Lemire and Nicolas[11] has

[a]Author to whom correspondence should be addressed. Electronic mail: hqmin@nju.edu.cn

 0001-4966/2011/130(2)/772/11/$30.00

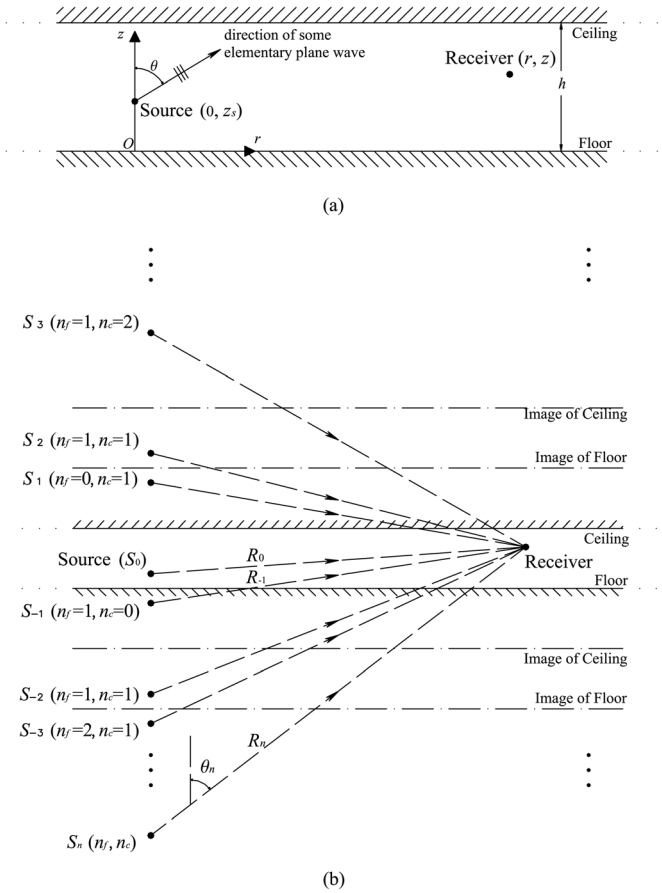

FIG. 1. Vertical section of a typical flat waveguide. (a) The source and receiver geometry, where the floor plane is $z=0$, the ceiling plane is $z=h$, and the horizontal distance between the source and receiver is r. (b) The schematic geometry of image sources, where the real source is assumed to be S_0. Each source leads a sound ray propagation path to the receiver with different reflection orders on the floor (n_f) and on the ceiling (n_c). R_n denote the propagation distance of the corresponding ray from the nth image source to the receiver and θ_n represents the separation angle between the vertical direction and propagation direction of the rays. Images of the ceiling and floor planes are also shown in the geometry to help better understand the reflections on the boundaries during propagation of the rays.

been the basis of coherent prediction models recently developed by Iu and Li,[17,18] Lam and Li,[19] and Law *et al.*[20] for sound field study in narrow street canyons, long spaces, and tunnels, respectively. Good accuracy from these models was observed in spaces with reflective boundaries. Unfortunately in the method of Lemire and Nicolas, it is implicitly assumed that the wave front shapes remain spherical after each successive reflection of the initial spherical wave incidence,[11] and this requires that the boundaries can be approximated as infinite and hard ones.[21,22] It would be interesting to investigate the accuracy degree of this method for spaces with absorbent boundaries, particularly when some of the boundaries are highly sound absorptive.

Westwood[23] has proposed a ray-based method for sound fields in flat waveguides with a penetrable bottom boundary and an idealized sound-soft top boundary to model the shallow water ocean environment. In his method, the multiple reflections of a spherical wave incidence on the interfaces were also formulated as integrals from plane wave expansion and then the integrals were evaluated numerically or with the first-order approximation similar to the method of Gensane and Santon.[15] Unfortunately, no further analytical solutions were given.

In review of these previous studies, there are needs of research toward a simple but accurate coherent model to predict the sound propagation in flat waveguides with a sound absorptive ceiling and a reflective floor, particularly at large distances from the source compared to the space height. This is the objective of this paper.

II. THEORETICAL METHOD

A. Formulation of the problem

Figure 1(a) shows a vertical section of a flat waveguide, where the infinite ceiling and floor planes are assumed to be locally reactive with uniform normalized specific admittance of β_c and β_f, respectively. The height between the ceiling and floor is h, a point source is located at $(0, z_S)$ and a receiver is at (r, z) with r being the horizontal distance from the source to receiver. The time-dependent factor $e^{-j\omega t}$ is suppressed for simplicity throughout this paper.

Based on the plane wave expansion of a spherical wave, the Green function in free field can be expressed as[14]

$$\frac{e^{jkR_0}}{4\pi R_0} = \frac{jk}{8\pi^2}\int_0^{2\pi}\int_0^{\pi/2-j\infty} e^{j\mathbf{k}\cdot\mathbf{R_0}} \sin\theta \, d\theta \, d\varphi, \tag{1}$$

where $\mathbf{k} = k(\sin\theta\cos\varphi,\ \sin\theta\sin\varphi,\ \cos\theta)$, k is the wave number, and $\mathbf{R_0}$ is the distance vector from the source to the receiver with a magnitude of R_0. The parameters θ and φ represent the azimuth angles characterizing the direction of each plane wave propagation in vertical and horizontal planes, respectively.

In the absence of the ceiling, the first reflection of the spherical wave incidence can be obtained by superposition of all the elementary plane wave reflections on the floor plane as[14]

$$P_{-1} = \frac{jk}{8\pi^2}\int_0^{2\pi}\int_0^{\pi/2-j\infty} e^{j\mathbf{k}\cdot\mathbf{R}_{-1}} V_f(\theta) \sin\theta \, d\theta \, d\varphi, \tag{2}$$

where P_{-1} denotes the field of the first reflection on the floor and $\mathbf{R_{-1}} = (R_{-1}\sin\theta_{-1}\cos\varphi_{-1},\ R_{-1}\sin\theta_{-1}\sin\varphi_{-1},\ R_{-1}\cos\theta_{-1})$ is the corresponding distance vector from the image source S_{-1} to the receiver, as shown in Fig. 1(b). $V_f(\theta)$ represents the plane wave reflection coefficient of the floor at the incidence angle θ and is given by

$$V_f(\theta) = \frac{\cos\theta - \beta_f}{\cos\theta + \beta_f}. \tag{3}$$

When the ceiling presents, the total field can be constructed with the rays from an infinite number of image sources,[14]

$$P_{\text{tot}} = \sum_{n=-\infty}^{+\infty} P_n, \tag{4}$$

in which $n = 0, \pm1, \pm2, \ldots$, and P_n represents the ray contribution from the nth image source, where a positive n is for

an image source located in the source series above the ceiling and a negative n is for that located below the floor as shown in Fig. 1(b). Particularly P_0 denotes the direct sound from the real source. Similar to Eq. (2), the ray contribution from the path with n_f floor reflections and n_c ceiling reflections can be expressed with an integral as[14]

$$P_n = \frac{jk}{8\pi^2}\int_0^{2\pi}\int_0^{\pi/2-j\infty} e^{j\mathbf{k}\cdot\mathbf{R_n}}[V_f(\theta)]^{n_f}[V_c(\theta)]^{n_c}\sin\theta d\theta d\varphi, \quad (5)$$

where $\mathbf{R_n} = (R_n\sin\theta_n\cos\varphi_n,\ R_n\sin\theta_n\sin\varphi_n,\ R_n\cos\theta_n)$ is the distance vector from the nth image source S_n to the receiver, θ_n and φ_n denote the azimuth angles to characterize the direction of $\mathbf{R_n}$ in vertical and horizontal planes, respectively. $V_c(\theta)$ is the plane wave reflection coefficient on the ceiling boundary,

$$V_c(\theta) = \frac{\cos\theta - \beta_c}{\cos\theta + \beta_c}. \quad (6)$$

The boundary reflection order n_f and n_c can be determined from the image source order n with a rule of

$$n_f = \frac{|n|}{2} - \frac{1}{2}\mathrm{sgn}(n)\mathrm{rem}(|n|,2), \quad (7a)$$

and

$$n_c = \frac{|n|}{2} + \frac{1}{2}\mathrm{sgn}(n)\mathrm{rem}(|n|,2), \quad (7b)$$

where $\mathrm{sgn}(\cdot)$ denotes the signum function that is $+1$ for the positive input and equals -1 for the negative input, and $\mathrm{rem}(|n|,2)$ represents the remainder of $|n|$ after division by 2.

Defining an overall coefficient $V(\theta)$ to replace the term $[V_f(\theta)]^{n_f}[V_c(\theta)]^{n_c}$ and using the geometrical identity of $r = R_n\sin\theta_n$, P_n in Eq. (5) is rewritten as

$$P_n = \frac{jk}{8\pi^2}\int_0^{2\pi}\int_0^{\pi/2-j\infty}\exp\Big\{jk[r\sin\theta(\cos\varphi\cos\varphi_n + \sin\varphi\sin\varphi_n) + R_n\cos\theta\cos\theta_n]\Big\}V(\theta)\sin\theta d\theta d\varphi, \quad (8)$$

and then can be further transformed into

$$P_n = \frac{jk}{8\pi^2}\int_0^{\pi/2-j\infty}\left\{\int_0^{2\pi}\exp[jkr\sin\theta\cos(\varphi-\varphi_n)]d\varphi\right\} \times \exp(R_n\cos\theta\cos\theta_n)V(\theta)\sin\theta d\theta. \quad (9)$$

As the function $V(\theta)$ is independent of integration variable φ, by using[14,24]

$$\int_0^{2\pi}\exp[jkr\sin\theta\cos(\varphi-\varphi_n)]d\varphi \equiv 2\pi J_0(kr\sin\theta), \quad (10)$$

where $J_0(\cdot)$ represents the Bessel function of the zeroth order, Eq. (9) can be simplified as

$$P_n = \frac{jk}{4\pi}\int_0^{\pi/2-j\infty}\exp[jkR_n\cos\theta\cos\theta_n]V(\theta)J_0(kr\sin\theta) \times \sin\theta d\theta. \quad (11)$$

Using the identities for a complex number u that $J_0(u) = [H_0^1(u) + H_0^2(u)]/2$ and $H_0^2(-u) = -H_0^1(u)$, Eq. (11) can be written as

$$P_n = \frac{jk}{8\pi}\int_{-\pi/2+j\infty}^{\pi/2-j\infty} V(\theta)\sin\theta H_0^1(kr\sin\theta) \times \exp[jkR_n\cos\theta\cos\theta_n]d\theta, \quad (12)$$

where $H_0^1(\cdot)$ and $H_0^2(\cdot)$ are the Hankel functions of the first and second kind with the zeroth order. Now the total field from a point source in a flat waveguide is explicitly formulated by Eq. (4) accompanied by the integral equation (12).

B. The coherent image source method

As shown in Fig. 1(b), P_0 is the direct sound $e^{jkR_0}/4\pi R_0$, and P_1 and P_{-1} are the fields of single reflections whose integral expressions with Eq. (12) can be evaluated with the exact (integral) solution provided by Nobile and Hayek,[25]

$$P_1 = \frac{e^{jkR_1}}{4\pi R_1}\left[1 - \frac{4jk\beta_c BR_1}{\beta_c + \cos\theta_1}I(k,R_1,\beta_c,\theta_1)\right], \quad (13a)$$

$$P_{-1} = \frac{e^{jkR_{-1}}}{4\pi R_{-1}}\left[1 - \frac{4jk\beta_f BR_{-1}}{\beta_f + \cos\theta_{-1}}I(k,R_{-1},\beta_f,\theta_{-1})\right], \quad (13b)$$

where $I(\cdot)$ is an integral function given by

$$I(k,R_n,\beta,\theta_n) = \int_0^\infty \frac{e^{-jkR_n(t^2+2Bt)}}{\sqrt{1 - t^2/H - 2Bt/H}}dt, \quad (14)$$

in which β is the normal specific admittance of the plane that the reflection takes place on

$$B = -j\sqrt{1 + \beta\cos\theta_n - (1-\beta^2)^{1/2}\sin\theta_n}, \quad (15a)$$

and

$$H = 1 + \beta\cos\theta_n + (1-\beta^2)^{1/2}\sin\theta_n. \quad (15b)$$

For the ray with multiple reflections ($|n| \geq 2$) on boundaries, although the exact solution of integral expression of P_n is generally not possible, it is feasible to approximate such integral analytically with the method of steepest descents for larger kr.[14,16] A second-order approximate solution provided by Brekhovskikh[14] in term of asymptotic series with accuracy to terms of $1/(kR_n)^2$ is

$$P_n = \frac{e^{jkR_n}}{4\pi R_n}V(\theta_n) - \frac{e^{jkR_n}}{4\pi R_n}\frac{j}{2kR_n}[V'(\theta_n)\cot\theta_n + V''(\theta_n)] + \cdots, \quad (16)$$

where $V'(\theta_n)$ and $V''(\theta_n)$ represent the first and second derivative of $V(\theta)$ at θ_n, respectively, and $V(\theta) = [V_f(\theta)]^{n_f}$

$[V_c(\theta)]^{n_c}$. Although Eq. (16) can be used in flat waveguides directly, its convergence needs to be analyzed before applications into the circumstance concerned in this paper. After substituting the expressions of $V_f(\theta)$ and $V_c(\theta)$ in Eqs. (3) and (6) into Eq. (16), a common factor of $[(\cos\theta_n+\beta_f)^{n_f}(\cos\theta_n+\beta_c)^{n_c}]^{-1}$ can be found in all series terms in Eq. (16).

In the current circumstance, the floor is acoustical reflective, which leads $|\beta_f|\to 0$. If a receiver is far from the source compared to the waveguide height, which is a situation often encountered in large open-plan offices, the incidence angle θ_n of rays at the first few orders whose contributions are significant in the total field, will approach $\pi/2$ as shown in Fig. 1(b). This causes $(\cos\theta_n+\beta_f)\to 0$, and then limits the convergence radius of the asymptotic series in Eq. (16). Hence the second-order approximation in Eq. (16) might not be sufficiently accurate for the current problem theoretically.

Using explicit higher orders of the asymptotic series in Eq. (16) to improve the approximation is not successful as the exponential complexity is encountered as the order increases[14,15] and such an extension appears not sensible when the common factor $[(\cos\theta_n+\beta_f)^{n_f}(\cos\theta_n+\beta_c)^{n_c}]^{-1}\to\infty$.[16] The steepest descent method modified by subtraction of the pole has been employed to remedy the similarly worsen accuracy of the asymptotic series for sound propagation along a single reflective boundary.[16,26] This modified method is based on the Laurent series expansion of the integrand in Eq. (2) to avoid the singularities from the poles. Nonetheless such a strategy becomes difficult in the case of flat waveguides with two boundaries, because the poles in this case come from the denominator $(\cos\theta+\beta_f)^{n_f}(\cos\theta+\beta_c)^{n_c}$ of the integrand in Eq. (12) and are mostly high order ones. It is intractable to explicitly obtain the residues of this integrand at these higher poles for Laurent series expansion.

Analysis on the physics of the problem might be helpful to overcome the mathematical intractability above and simplifies the problem. The solution in Eq. (13a) or (13b) for the singly reflected field from a point source on an infinite plane can be rewritten for generality with a form of image source method as

$$P_{\rm sr}=P_{\rm dis}Q_{\rm sr}, \tag{17}$$

where $P_{\rm sr}$ is the single reflection field of a spherical wave incidence on an infinite plane, $P_{\rm dis}$ is the direct field at the receiver from the image source due to the single perfect reflection, and $Q_{\rm sr}$ is the single reflection coefficient for spherical wave incidence, and can be determined from Eq. (13a) or (13b) by

$$Q_{\rm sr}=1-\frac{4jk\beta BR_n}{\beta+\cos\theta_0}I(k,R_n,\beta,\theta_n), \tag{18}$$

where R_n implies the propagation distance of the ray and interpretations of other parameters are in accord with those in Eqs. (13a), (13b), and (14).

It has been shown that the reflected wave of the spherical sound incidence from a point source remains almost spherical along a sufficiently hard boundary.[22] The wave front shapes of $P_{\rm dis}$ or $P_{\rm sr}$, which may be regarded as the spatial distribution of wave energy propagation in the time domain, can always be described as a function of the direction characterized with the incident angle θ_n from the image source to different spatial locations (receivers). From Eq. (17), the phenomenon that the wave front shape of $P_{\rm sr}$ is almost the same as that of $P_{\rm dis}$, requires a reflection coefficient $Q_{\rm sr}$ that is almost the same for different spatial parts of the wave front of $P_{\rm dis}$ for field phase shift during the reflection, namely, to require $Q_{\rm sr}$ being weakly dependent on θ_n. This indicates that the coefficient $Q_{\rm sr}$ can be assumed to be uniform for different spatial parts of incident wave fronts in the reflection on a hard boundary, no matter what shape the incident wave fronts are. Thus, according to Eq. (17), each reflection of a ray on a reflective boundary that is denoted by RB, regardless of the reflection being the first or the successive one in the ray propagation from the spherical radiation, can be heuristically approximated by

$$P_r\approx P_{\rm rp}Q_{\rm ref}({\rm IS},R|{\rm RB}), \tag{19}$$

where P_r denotes the ray field at receiver after a reflection on RB, and $P_{\rm rp}$ represents the expected ray field at the receiver if the boundary RB is rigid, which is just the perfectly reflected field on this boundary. $Q_{\rm ref}({\rm IS},R|{\rm RB})$, determined by Eq. (18) also, is used to replace the single reflection coefficient $Q_{\rm sr}$ for reflections on the reflective boundary RB and corresponds to the ray from the image source IS to receiver R. Equation (19) shows that each reflection of a ray on a reflective boundary can be evaluated by multiplying the corresponding perfectly reflected field with the spherical wave reflection coefficient on this boundary.

In the current circumstances, the floor boundary is reflective. Thus, before and after each reflection on it, the wave front shape can be assumed to remain the same. The ray field alterations after each reflection on it can be quantified by a weighting factor $Q_{\rm ref}({\rm IS},R|{\rm FB})$ that depends on the floor boundary (FB) and the ray geometry according to Eq. (19). Therefore in the propagation of a ray with reflection order n_f on the floor and n_c on the ceiling shown in Fig. 1(b), after each "transmission" through the floor or its images, the propagation field of the ray can be once weighted by the reflection coefficient $Q_{\rm ref}(S_n,R|{\rm FB})$. After the ray field being weighted for n_f times due to transmission through the floor and its images in propagation, the field contribution of the ray, P_n, can be approximated as

$$P_n\approx[Q_{\rm ref}(S_n,R|{\rm FB})]^{n_f}\frac{jk}{8\pi}\int_{-\pi/2+j\infty}^{\pi/2-j\infty}[V_c(\theta)]^{n_c}\sin\theta H_0^1 \times(kr\sin\theta)\exp(jkR_n\cos\theta\cos\theta_n)d\theta, \tag{20}$$

where $Q_{\rm ref}(S_n,R|{\rm FB})$ can be determined from Eq. (18). Being compared to Eq. (12), the integral of P_n in Eq. (20) has been simplified, and now the integrand involves only the reflection coefficient on the ceiling.

The integral in Eq. (20) describes the field of the ray after n_c times reflections on the absorbent ceiling. This can be evaluated by the second-order approximation in Eq. (16) with ensured accuracy because $|\beta_c|$ does not approach zero and for the asymptotic series there is no singularity similar to that from $(\cos\theta_n+\beta_f)\to 0$ when $\theta_n\to\pi/2$. So P_n can be further approximated for larger kr by

$$P_n \approx [Q_{\text{ref}}(S_n, R|\text{FB})]^{n_f} \left\{ V_t(\theta_n|\text{CB}, n_c) - \frac{j\left[V_t'(\theta_n|\text{CB}, n_c)\cot\theta_n + V_t''(\theta_n|\text{CB}, n_c)\right]}{2kR_n} \right\} \frac{e^{jkR_n}}{4\pi R_n}, \tag{21}$$

where $V_t(\theta|\text{CB}, n_c)$ represents a total plane wave reflection coefficient to take account of the successive n_c times plane wave reflections on the absorbent ceiling boundary (CB) at an incident angle θ, which equals $[V_c(\theta)]^{n_c}$ here. $V_t'(\theta_n|\text{CB}, n_c)$ and $V_t''(\theta_n|\text{CB}, n_c)$ are the first and second derivatives of $V_t(\theta|\text{CB}, n_c)$ at θ_n, respectively. The factor $e^{jkR_n}/4\pi R_n$ is the direct sound field at the receiver from the nth image source, while the factors in front of it act like a combined reflection coefficient to evaluate the overall influence from all the successive reflections during the ray propagation. Hence P_n can be expressed as

$$P_n = Q_n \frac{e^{jkR_n}}{4\pi R_n}, \tag{22}$$

where Q_n denotes the combined reflection coefficient corresponding to the ray with reflection order n as

$$Q_n = [Q_{\text{ref}}(S_n, R|\text{FB})]^{n_f} Q_{\text{abs}}(S_n, R|\text{CB}, n_c), \tag{23}$$

in which $Q_{\text{abs}}(S_n, R|\text{CB}, n_c)$ represents an overall reflection coefficient taking account of all the successive reflections on an absorbent boundary for a ray with spherical radiation, where n_c times successive reflections have taken place on the absorbent ceiling during the propagation of the ray from S_n to R. The coefficient $Q_{\text{abs}}(S_n, R|\text{CB}, n_c)$ can be approximated by

$$Q_{\text{abs}}(S_n, R|\text{CB}, n_c) \approx V_t(\theta_n|\text{CB}, n_c) - \frac{j\left[V_t'(\theta_n|\text{CB}, n_c)\cot\theta_n + V_t''(\theta_n|\text{CB}, n_c)\right]}{2kR_n}, \tag{24}$$

and $V_t(\theta|\text{CB}, n_c) = [V_c(\theta)]^{n_c}$.

Equations (22) and (23) are the main contribution of this paper, which in company with Eq. (4), deliver a coherent image source method to solve approximately the total field from a point source in flat waveguides with a sound absorptive ceiling and a reflective floor. On the basis of asymptotic approximations by the steepest descent method for large kr and a physically plausible assumption that wave front shape remains the same before and after each reflection on a sufficiently hard boundary, the solution has no other limitations in principle. In the next section, numerical simulations will be carried out to validate the model and compare it to the existing coherent ray-based methods.

III. NUMERICAL RESULTS AND DISCUSSIONS

The wave theory is a classical method to study sound fields in spaces with regular shape allowing separation of variables.[27,28] Although it is hard to be extended to the realistic enclosures with irregular shape,[11,29] the wave theory is analytically exact and can be used as a reference to validate the ray-based methods applied to the flat waveguides in this paper. The equations used in the wave theory to solve the sound field from a point source in flat waveguides are detailed in Appendix A. In the simulations, a general approach[30] for solving complex transcendental equations has been employed to numerically solve the eigenvalue equation [Eq. (A6)] for absorbent boundaries. Moreover it is assumed in this paper that the high-order modes with an eigenvalue amplitude larger than 1.5 times of the actuating wave number can be neglected in total field computations in Eq. (A1) with the wave theory. A corresponding description and discussion on the evaluation with the wave theory are given in Appendix A in detail. For implementation of the image source methods in simulations, the locations of image sources can be determined through Fig. 1(b). The maximum image source order l for truncation is determined when the amplitude of the total energy field accumulated differs less than 0.1% from that accumulated at the order $l-10$.

To represent a realistic circumstance of open-plan offices in simulations, the ceiling of the flat waveguide is assumed to be a suspended one where a layer of homogeneous porous absorbent material is backed by a cavity of certain depth L. For simplicity, the backing cavity is assumed to be divided with partitions permitting the sound propagation in the cavity to be normal to the ceiling surface. The floor is assumed to be a simplified wooden one that is made up of a single homogeneous wood layer with an acoustically hard backing. The evaluation of surface admittances for the suspended ceiling and the wooden floor is detailed in Appendix B, where the media parameters of the ceiling porous material layer or the floor wood layer, flow resistivity (σ), porosity (Ω), tortuosity (T), pore shape factor (S_p), and thickness (d), are used for description. Figure 2 shows the normal incident absorption coefficient of the ceilings and floor used in simulations hereafter as a function of frequency.

Two numerical cases are investigated to access the prediction performance with the proposed method and the existing coherent ray-based methods in flat waveguides, such as the method of Brekhovskikh,[14] the method of Lemire and Nicolas,[11] and the method of Gensane and Santon.[15] In the simulations, the method of Lemire and Nicolas[11] is modified

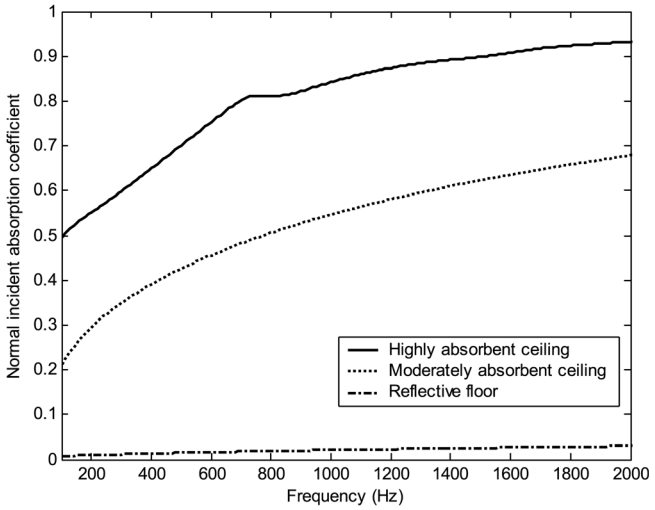

FIG. 2. Spectra of normal incident absorption coefficient of three types of boundaries used in the numerical simulations, where the highly absorbent ceiling is defined by $\sigma = 30$ cgs, $\Omega = 1$, $T = 1$, $S_p = 0.25$, $d = 0.1$ m, and $L = 0.2$ m, whereas the moderately absorbent one is defined with the same parameters except that $\sigma = 150$ cgs. The floor is assumed to be a reflective wooden one with parameters of $\sigma = 10\,000$ cgs, $\Omega = 0.2$, $T = 1.4$, $S_p = 0.5$, and $d = 0.01$ m.

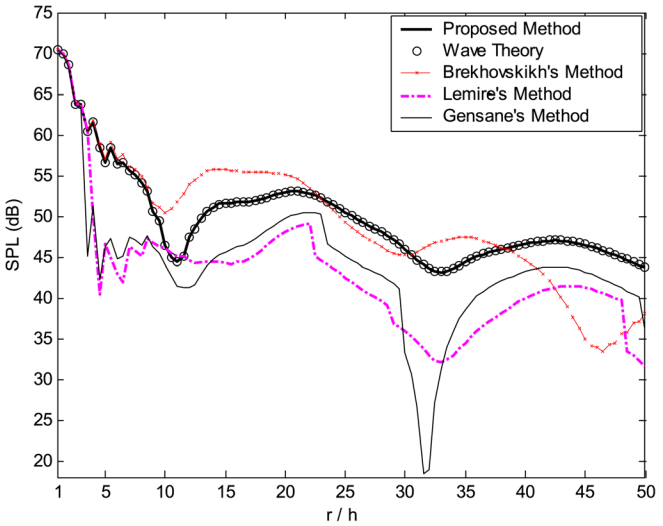

FIG. 3. (Color online) Predictions of the sound pressure levels (SPLs) at frequency 1000 Hz vs the horizontal distance (r) between the source and receiver in a flat waveguide with height (h) of 2 m, where all the source and receivers are located at 0.25 m above the floor. The ceiling is the highly sound absorbent type and the floor is reflective. The solid line represents the results with the proposed method, the circles are those in the wave theory, the dashed line with cross markers is with the ray method from Brekhovskikh (Ref. 14) (Brekhovskikh's method), the dash-dotted line is from the modified method of Lemire and Nicolas (Ref. 11) (Lemire's method), and the dotted line is with the method of Gensane and Santon (Ref. 15) (Gensane's method).

by replacing the approximate spherical wave reflection coefficient employed in it, the term $R_p + (1 - R_p)F(\omega)$, in Eq. (7) of Ref. 11, with the exact integral one in Eq. (18) proposed by Nobile and Hayek[25] for better accuracy and applicability.[11,25] The ceiling of the flat waveguide is assumed to be highly sound absorptive in the first case and to be moderately absorptive in the second, whereas the floor keeps reflective and the waveguide height is always 2 m unless otherwise stated.

In the first case, parameters of the porous material in the suspended ceiling are $\sigma = 30$ cgs (where 1 cgs = 1 kPa s m^{-2}), $\Omega = 1$, $T = 1$, $S_p = 0.25$, and $d = 0.1$ m to represent a highly sound absorptive wool layer[31] and the backing cavity depth L is 0.2 m. The selected parameters of the floor wood layer are $\sigma = 10\,000$ cgs, $\Omega = 0.2$, $T = 1.4$, $S_p = 0.5$, and $d = 0.01$ m to represent a high density wooden flooring.[31,32] The predictions of the sound pressure level (SPL) are first investigated versus the horizontal distance between the source and receiver at 1 000 Hz, where heights of the source and receivers are chosen to be 0.25 m and the normal incident absorption coefficients of the ceiling and floor are 0.84 and 0.02 respectively.

The corresponding results with the proposed method, the wave theory, and the exiting ray-based methods are compared in Fig. 3. It can be seen that the results from the proposed method and those from the wave theory almost overlap over the range of r/h from 1 to 50. The method of Gensane and Santon[15] provides accurate results only when the horizontal distance between the source and receiver is smaller than two times of the waveguide height, and the modified method of Lemire and Nicolas[11] is accurate with r/h below 3. Although the method of Brekhovskikh,[14] which is the second-order approximate solution in Eq. (16) for the flat waveguide, predicts much better than the latter two existing image source methods, large discrepancies are found between the results from it and those from the wave theory after r becomes larger than 8 times that of h. This indicates that when receivers are far away from the source compared to the height of flat waveguides, the existing coherent ray-based methods are hard to predict the sound propagation accurately. On the other hand, the excellent prediction agreement between the existing ray-based methods and the wave theory at receivers rather close to the source provides cross-validation for the numerical calculations with the wave theory at the receivers far from the source, because the eigenvalues

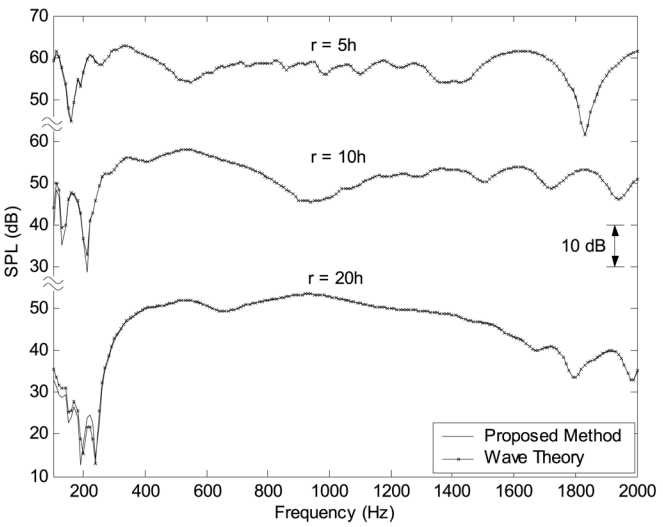

FIG. 4. Spectra of sound pressure levels (SPLs) in a flat waveguide with height (h) of 2 m, where the source is located at (0, 0.25 m) and receivers are at (r, 0.25 m) and pairs of results corresponding to different source/receiver distances are shifted to fit on a single figure. The ceiling is the highly sound absorbent type and the floor is reflective. The solid lines represent the results with the proposed method, and the dotted lines with cross markers are those in the wave theory.

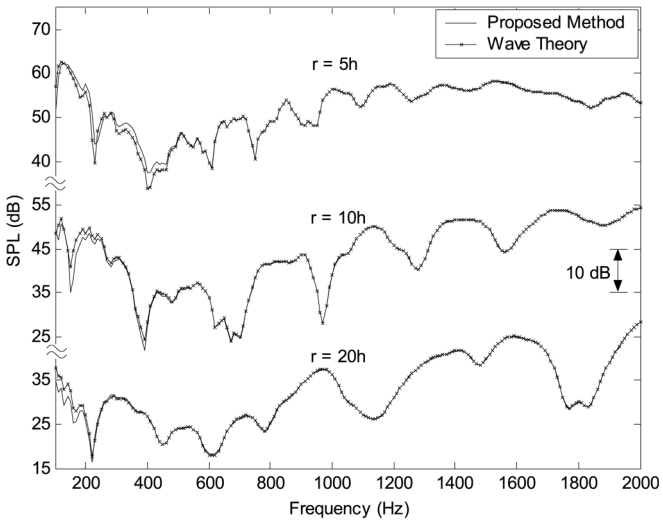

FIG. 5. Same caption as Fig. 4 except that the height of the source and receivers becomes 1.8 m.

from the wave theory solution at a given frequency are exactly the same for the sound field at different receivers.

Computations have been carried out in this case to further validate the proposed method in the frequency range from 100 to 2 000 Hz, where receivers are chosen with a set of horizontal distances from the source of 5, 10, and 20 times of the waveguide height. Figures 4 and 5 show the results corresponding to the situations where the source and receivers are close to the sound reflective floor ($z_s = z = 0.25$ m) or the absorbent ceiling ($z_s = z = 1.8$ m), respectively, so as to simulate the propagation of noise from the floor-standing electrical appliances or the ceiling-mounted ventilation devices in usual open-plan offices. The situation for sound propagations at the height of a seated person ($z_s = z = 1.2$ m) is also investigated and the corresponding results are presented in Fig. 6.

As shown from Figs. 4–6, the prediction of SPLs with the proposed method always agree well with the wave theory over a broad frequency range, except small differences observed at some lower audio frequencies, which may be explained with two reasons. First the accuracy of Eq. (16) is ensured in theory for large kr. Second at these low frequencies, the magnitude of β_c becomes small from the evaluation by the surface admittance model in Eqs. (B1), (B3a), and (B3b). This leads to large $(\cos\theta_n + \beta_c)^{-1}$ in the common factor of the series in Eq. (24), as well as large $(\cos\theta_n + \beta_f)^{-1}$ for the series in Eq. (16) as $\theta_n \to \pi/2$, which can reduce the degree of approximation for $Q_{\text{abs}}(S_n, R|\text{CB}, n_c)$ significantly.

In the second numerical case, the ceiling is defined with the same parameters used in the first case except that the flow resistivity σ of the porous material changes to be 150 cgs. The parameters of the floor are the same with those in the first case. The corresponding SPL vs r/h curves predicted with the proposed method, the wave theory, and the existing ray-based methods are compared in Fig. 7, where $z_S = z = 0.25$ m and the frequency is 1 000 Hz still for examination, whereas the normal incident absorption coefficient of the ceiling becomes 0.55.

In Fig. 7, the agreement between the proposed method and the wave theory is remarkably good with r/h ranging from 1 to 50. The method of Brekhovskikh[14] is shown with errors for an r/h ratio larger than 7, whereas the performance from the methods of Lemire and Nicolas[11] and Gensane and Santon[15] seems better by comparison with that in Fig. 3 of the first case, which might be explained by less wave front shape distortion after each reflection on the ceiling as it is less absorbent. In this case, the spectra of SPL in the frequency range from 100 to 2 000 Hz, predicted with the proposed method and the wave theory, are also compared with the same considerations on source/receiver geometries in the first case. The results corresponding to the situation where $z_s = z = 1.2$ m are presented in Fig. 8, which shows that predictions from the proposed method are in good agreement with the reference method over a broad frequency range again, except small differences at some low frequencies.

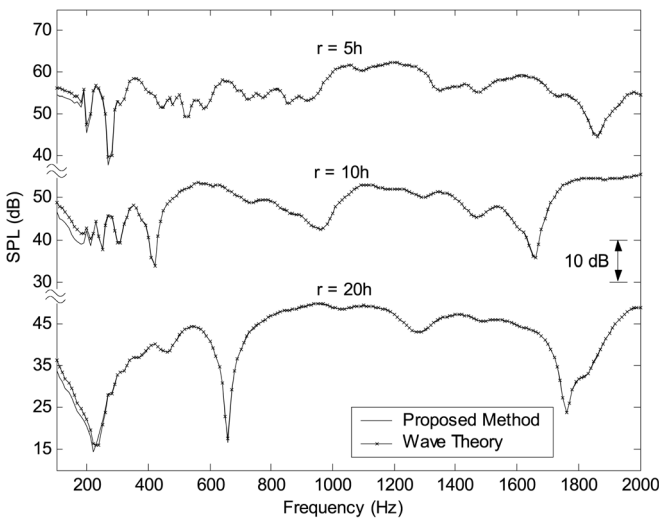

FIG. 6. Same caption as Fig. 4 except that the height of the source and receivers becomes 1.2 m.

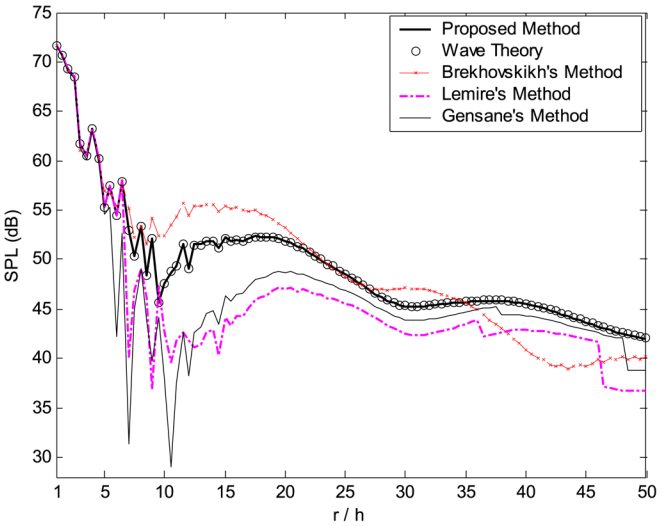

FIG. 7. (Color online) Same caption as Fig. 3 except that the ceiling becomes the moderately sound absorbent type.

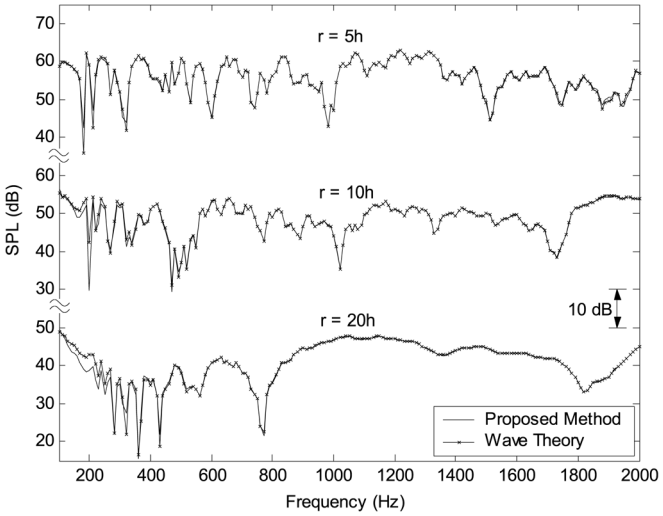

FIG. 8. Spectra of sound pressure levels (SPLs) in a flat waveguide with height (h) of 2 m, where the source is located at (0, 1.2 m) and receivers are at (r, 1.2 m) and pairs of results corresponding to different source/receiver distances are shifted to fit on a single figure. The ceiling is the moderately sound absorbent type and the floor is reflective. The solid lines represent the results with the proposed method, and the dotted lines with cross markers are those in the wave theory.

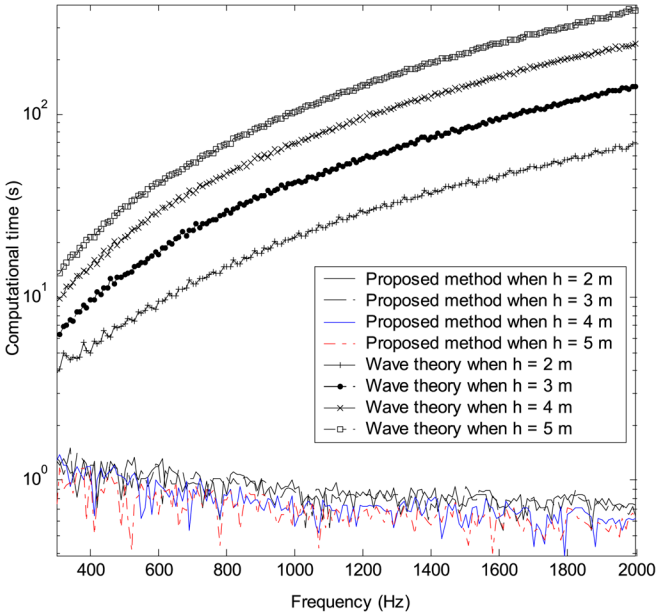

FIG. 9. (Color online) Spectra of the computational time with the proposed method and the numerical evaluation of the wave theory to predict the sound fields in flat waveguides with different heights (h) from 2 to 5 m, where the source is located at (0, 0.25 m) and receivers are at ($5h$, 0.25 m). The ceiling is the highly sound absorbent type and the floor is reflective. The lines represent the computational time results with the proposed method, and the lines with markers are those with the wave theory.

More similar results were obtained by selecting other source/receiver geometries and other parameters of the ceiling and floor extensively, but they are not presented here for reasons of brevity. These results support that the proposed method is valid for predicting the sound propagation in flat waveguides with a sound absorptive ceiling and a reflective floor over a broad frequency range, even at large distances from the source compared to the space height while the ceiling can be highly sound absorptive.

The computational time with the proposed method is also investigated versus the frequency and the space height, by comparison to that from the numerical evaluation of the wave theory. The boundary parameters in the first numerical case are used for these investigations and the waveguide height is assumed to be 2, 3, 4, and 5 m in sequence. The location of source is (0, 0.25 m) and those of receivers are ($5h$, 0.25 m). The corresponding computational time with these two methods in the frequency range from 300 to 2 000 Hz with different space heights are presented in Fig. 9. It is shown that the computational time with the wave theory increases remarkably as the actuating frequency increasing, whereas the general trend of that with the proposed method is observed to be a little decrease at higher frequencies, despite of fluctuations that may be due to field coherence between different reflected waves during truncating image source series at single frequencies.

Numerical results presented in Fig. 10 may explain the frequency dependence of computational time with the wave theory, which are carried out to validate the convergence of the total field computations in Eq. (A1). It is indicated from Fig. 10 that more eigenvalue roots in Eq. (A6) are needed to be found to include more high-order modes into total field computation at higher frequencies for convergence, which increases the computational time with the wave theory. However for the proposed image source method, generally less image source orders are needed for convergence at higher frequencies as the boundaries lined with porous materials become more acoustically absorbent at higher frequencies as shown in Fig. 2.

From Fig. 9, it is also shown that with larger space heights, more computational time is needed for the evaluation of the wave theory, but a little less time is needed for the calculation of the proposed method. This is because larger space

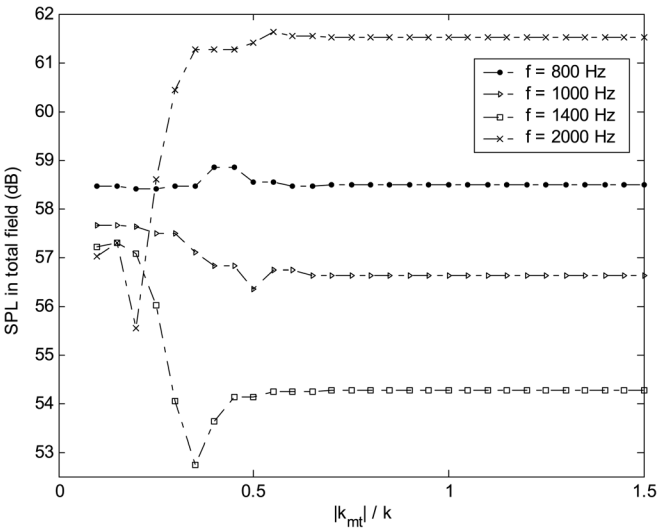

FIG. 10. The convergence of sound pressure level (SPL) in the total field evaluated with the wave theory vs the maximum eigenvalue amplitude ($|k_{mt}|$) in truncating the infinite mode series in total field computations in Eq. (A1) at four different actuating frequencies (f), where k is the actuating wave number. The flat waveguide is 2 m high, the source is located at (0, 0.25 m) and the receiver is at (10 m, 0.25 m). The ceiling is the highly sound absorbent type and the floor is reflective.

dimensions lead to higher distribution density of the eigenvalue roots in a given interval with the wave theory,[27,28] but they cause faster energy fading of the image sources in the proposed method due to geometric attenuation. It should be noted that the evaluation of the wave theory may be speeded up with some other numerical methods[33] or other configurations. Nevertheless, it is indicated from Fig. 9 that for predicting the sound fields in the flat waveguides with absorbent boundaries, the proposed method is preferable to the wave theory at higher frequencies and for spaces with larger dimensions.

From the above-mentioned results for sound fields in flat waveguides with a sound absorptive ceiling and a reflective floor, it is clear that the proposed coherent image source method is valid and can provide more accurate predictions than the existing coherent ray-based methods for various source/receiver geometries. Although it is found from the numerical results that the proposed method can have reasonable accuracy at certain low frequencies, it must be remarked that the method is based on two assumptions: (i) kr being large and (ii) wave front shape remaining the same before and after each reflection on a reflective boundary. Moreover, numerical results validate the idea proposed in Eq. (23) of separating the reflections on the reflective boundaries from those on absorbent ones in applying reflection coefficients in the image source method. This idea is expected to be useful for developing an accurate and versatile coherent image source method for sound fields in practical enclosures with absorbent boundaries.

IV. CONCLUSION

An accurate coherent image source method has been proposed in this paper to predict single frequency sound propagation in flat waveguides with a sound absorptive ceiling and a reflective floor. By expending a spherical wave into plane wave integrals, the method avoids the intractability in analytically evaluating the integrals of reflection waves. This is achieved by introducing a physically plausible assumption that wave front shapes remain the same before and after each reflection on a reflective boundary. The proposed coherent model can be used to predict sound propagation from a point source to arbitrary receiver locations in flat waveguides with highly absorptive ceiling. The method has been numerically validated with the wave theory for various source/receiver geometries over a broad frequency range. It is shown that the proposed method can accurately predict the single frequency sound propagation, even if at large distances from the source compared to the waveguide height whereas the existing coherent ray-based method are inaccurate. It is also shown that the proposed method is preferable to the wave theory at higher frequencies and with larger space dimensions. The proposed method should be useful for sound field prediction in open-plan offices.

ACKNOWLEDGMENTS

The authors are grateful to Dr. Hongjie Pu and Yan Chen for the valuable discussions. They also appreciate the anonymous reviewers for useful comments. This work is partially supported by Natural Science Foundation of China (Project No. 11004101) and the Fundamental Research Funds for the Central Universities (Project No. 1093020403).

APPENDIX A: THE WAVE THEORY SOLUTION FOR THE SOUND FIELD FROM A POINT SOURCE IN FLAT WAVEGUIDES

Based on the wave theory in Refs. 27 and 28, the sound field from a point source in flat waveguides can be solved as a summation of normal modes along directions z and r in Fig. 1(a). It is expressed as[27,28]

$$P_{\text{tot}} = \frac{jA}{4}\sum_{m=0}^{\infty}\frac{\psi_m(z_S)\psi_m(z)}{||\psi_m||^2}H_0^1(K_r r), \tag{A1}$$

where A is the amplitude of the point source and assumed to be unit, z_S and z are heights of the source and receiver, respectively, and r denotes the source/receiver horizontal distance. The term $||\psi_m||^2$ represents the norm of the eigenfunction $\psi_m(\cdot)$:

$$||\psi_m||^2 = \int_0^h [\psi_m(z)]^2 dz. \tag{A2}$$

The eigenfunction $\psi_m(.)$ can be expressed as

$$\psi_m(z) = e^{jk_m z} + \gamma_m e^{-jk_m z}, \tag{A3}$$

where k_m denotes the eigenvalue in the z direction and γ_m is a complex constant related to k_m. Correspondingly the wave number in the r direction in Eq. (A1), K_r, is determined from k_m by

$$K_r = +\sqrt{k^2 - k_m^2}, \tag{A4}$$

where the complex square root is taken to yield a result with a positive real part and k is the wave number. The eigenvalue k_m and constant γ_m are obtained from the boundary condition equations along the pair of planes in the posed problem, which are

$$\begin{cases} \dfrac{\partial\psi_m(0)}{\partial z} + jk\beta_f\psi_m(0) = 0 \text{ on the floor boundary} \\ \dfrac{\partial\psi_m(h)}{\partial z} - jk\beta_c\psi_m(h) = 0 \text{ on the ceiling boundary.} \end{cases} \tag{A5}$$

Hence the eigenvalue equations can be obtained as

$$\frac{k_m + k\beta_f}{k_m - k\beta_f}\frac{k_m + k\beta_c}{k_m - k\beta_c} = e^{2jhk_m}, \tag{A6}$$

and

$$\gamma_m = \frac{k_m + k\beta_f}{k_m - k\beta_f}. \tag{A7}$$

It should be noted that the analytical solution of Eq. (A6) is available only if the boundaries are rigid. For boundaries with complex admittance, transcendental equation (A6) becomes complex and may be solved by approximations[27,28] or classical numerical approaches, such as Newton's iteration if the boundaries are nearly rigid with sufficiently low admittance amplitude.[33] When boundaries are absorbent with large admittance amplitude, the number of eigenvalue roots in Eq. (A6) and their possible locations in a given interval become hard to know,[33] to which the classical numerical methods in solving nonlinear equations become inapplicable because they need one "good" single initial guess to yield a root. To ensure high accuracy of evaluation with the wave theory as a validation benchmark, a general numerical scheme[30] can be used to solve all the eigenvalue roots in Eq. (A6) in a given interval with robustness, which avoids selecting the initial guesses in eigenvalue solution.

The solution in Eq. (A1) is expressed as the superposition of an infinite mode series, which however can be truncated at a finite number of modes in practice.[33] To validate the truncation criterion considered in this paper for convergence of the total field computations, sound pressure levels in the total field at frequencies of 800, 1000, 1400, and 2000 Hz are examined versus the maximum eigenvalue amplitude $|k_{mt}|$ considered for truncating the infinite mode series. The corresponding results based on parameters in the first numerical case in Sec. III are presented in Fig. 10, which show that the total field becomes convergent with $|k_{mt}|$ larger than about 0.6 times of the actuating wave number k at different frequencies. Therefore $|k_{mt}|$ is chosen to be 1.5 times k in this paper to ensure high evaluation accuracy of the wave theory as a reference method.

APPENDIX B: EVALUATION OF BOUNDARY SURFACE ADMITTANCE FOR THE CEILING AND FLOOR

The surface admittance of the suspended ceiling, β_c, and that of the wooden floor, β_f, can be evaluated, respectively, according to classic electrical transmission line analogy,[32]

$$\beta_c = \frac{Z_a + jZ_L \tan(k_a d)}{Z_a[Z_L + jZ_a \tan(k_a d)]}, \tag{B1}$$

and

$$\beta_f = \frac{1}{Z_a \coth(jk_a d)}, \tag{B2}$$

where Z_L in Eq. (B1) represents the specific characteristic impedance of the backing cavity in the ceiling and can be $-j/\tan(2\pi fL/c)$ in this paper, in which f is the frequency of interest, L denotes the cavity depth, and c is the sound velocity in air. Parameter d represents the thickness of the ceiling porous material layer in Eq. (B1) or the floor wood layer in Eq. (B2). Z_a and k_a denote, respectively, the specific characteristic impedance and the propagation constant inside the ceiling porous material in Eq. (B1) or inside the floor wood layer in Eq. (B2), which can be evaluated by Attenborough's "three-parameter" approximation[32]

$$Z_a = \left(\frac{4T}{3\Omega} - \frac{4j\Omega\sigma_e}{2\pi f\rho_0}\right)\left(\frac{2\pi f}{ck_a}\right), \tag{B3a}$$

$$k_a = \frac{2\pi f}{c}\sqrt{\gamma\left(aT - \frac{4j\Omega^2\sigma_e}{2\pi f\rho_0}\right)}, \tag{B3b}$$

where Ω and T are the porosity and tortuosity inside the media, respectively. ρ_0 and γ denote the density and the ratio of specific heats for air separately, where $\rho_0 = 1.293$ kg m^{-3}and $\gamma = 1.4$ in simulations at the room temperature. Parameter a inside Eq. (B3b) is defined by $a = 4/3 - [(\gamma - 1)/\gamma]N_{\mathrm{Pr}}$, where N_{Pr} is the Prandtl number for air and can be 0.71 at the room temperature. In Eqs. (B3a) and (B3b), σ_e denotes an effective flow resistivity and is defined by $\sigma_e = 4S_p^2\sigma/\Omega$, where S_p is the pore shape factor and σ is the flow resistivity of the media with a unit of cgs (1 cgs = 1 kPa s m^{-2}).

[1] M. Asselineau, "Noise control of laboratories: case studies," Proceedings of Acoustics 08 Paris, 2008, pp. 5165–5169.
[2] D. A. Bies and C. H. Hansen, *Engineering Noise Control Theory and Practice*, 3rd ed. (E&FN SPON, London, 2006), pp. 314–324.
[3] E. A. Lindqvist, "Sound attenuation in larger factory spaces," Acustica. **50**, 313–328 (1982).
[4] M. Hodgson, "On the prediction of sound fields in large empty rooms," J. Acoust. Soc. Am. **84**, 253–261 (1988).
[5] M. Hodgson, "On the accuracy of models for predicting sound propagation in fitted rooms," J. Acoust. Soc. Am. **88**, 871–878 (1990).
[6] S. M. Dance and B. M. Shield, "The complete image-source method for the prediction of sound distribution in non-diffuse enclosed spaces," J. Sound Vib. **201**, 473–489 (1997).
[7] A. M. Ondet and J. L. Barbry, "Modeling of sound propagation in fitted workshops using ray tracing," J. Acoust. Soc. Am. **85**, 787–796 (1989).
[8] M. Hodgson, "Ray-tracing evaluation of empirical models for predicting noise in industrial workshops," Appl. Acoust. **64**, 1033–1048 (2003).
[9] J. Kang, "Numerical modeling of the speech intelligibility in dining spaces," Appl. Acoust. **63**, 1315–1333 (2002).
[10] S. M. Dance, J. P. Roberts, and B. M. Shield, "Computer prediction of sound distribution in enclosed spaces using an interference pressure model," Appl. Acoust. **44**, 53–65 (1995).
[11] G. Lemire and J. Nicolas, "Aerial propagation of spherical sound waves in bounded spaces," J. Acoust. Soc. Am. **85**, 1845–1853 (1989).
[12] R. Pirn, "Acoustical variables in open planning," J. Acoust. Soc. Am. **49**, 1340–1345 (1971).
[13] C. Wang and J. S. Bradley, "A mathematical model for a single screen barrier in open-plan offices," Appl. Acoust. **63**, 849–866 (2002).
[14] I. Brekhovskikh, *Waves in Layered Media*, 2nd ed. (Academic, New York, 1980), pp. 225–320.
[15] M. Gensane and F. Santon, "Prediction of sound fields in rooms of arbitrary shape: validity of the image sources method," J. Sound Vib. **63**, 97–108 (1979).
[16] K. Attenborough, S. I. Hayek, and J. M. Lawther, "Propagation of sound above a porous half space," J. Acoust. Soc. Am. **68**, 1493–1501 (1980).
[17] K. K. Iu and K. M. Li, "The propagation of sound in narrow street canyons," J. Acoust. Soc. Am. **112**, 537–550 (2002).
[18] K. M. Ii and K. K. Iu, "Propagation of sound in long enclosures," J. Acoust. Soc. Am. **116**, 2759–2770 (2004).
[19] P. M. Lam and K. M. Li, "A coherent model for predicting noise reduction in long enclosures with impedance discontinuities," J. Sound Vib. **299**, 559–574 (2007).

[20]M. K. Law, K. M. Li and C. W. Leung, "Noise reduction in tunnels by hard rough surfaces," J. Acoust. Soc. Am. **124**, 961–972 (2008).
[21]J. B. Allen and D. A. Berkley, "Image method for efficiently simulating small-room acoustics," J. Acoust. Soc. Am. **65**, 943–950 (1979).
[22]U. Ingard, "On the reflection of a spherical sound wave from an infinite plane," J. Acoust. Soc. Am. **23**, 329–335 (1951).
[23]E. K. Westwood, "Ray methods for flat and sloping shallow-water waveguides," J. Acoust. Soc. Am. **85**, 1885–1894 (1989).
[24]S. Hassani, *Mathematical Physics: A Modern Introduction to its Foundations* (Springer, New York, 1999), pp. 438–442.
[25]M. A. Nobile and S. I. Hayek, "Acoustic propagation over an impedance plane," J. Acoust. Soc. Am. **78**, 1325–1336 (1985).
[26]C. F. Chien and W. W. Soroka, "Sound propagation along an impedance plane," J. Sound Vib. **43**, 9–20 (1975).
[27]H. Kuttruff, *Room Acoustics*, 5th ed. (Taylor & Francis, New York, 2009), pp. 67–91.
[28]P. M. Morse and K. U. Ingard, *Theoretical Acoustics* (McGraw-Hill, New York, 1968), pp. 492–509.
[29]M. Willatzen and L. C. Lew Yan Voon, "Eigenmodes of triaxial ellipsoidal acoustical cavities with mixed boundary conditions," J. Acoust. Soc. Am. **116**, 3279–3283 (2004).
[30]Y. Long and H. Jiang, "Rigorous numerical solution to complex transcendental equations," Int J. Infrared Milli. **19**, 785–790 (1998).
[31]K. Attenborough, "Acoustical characteristics of rigid fibrous absorbents and granular materials," J. Acoust. Soc. Am. **73**, 785–799 (1983).
[32]K. Attenborough, "Ground parameter information for propagation modeling," J. Acoust. Soc. Am. **92**, 418–427 (1992).
[33]Y. Naka, A. A. Oberai, and B. G. Shinn-Cunningham, "Acoustic engenvalues of rectangular rooms with arbitrary wall impedances using the interval Newton/generalized bisection method," J. Acoust. Soc. Am. **118**, 3662–3671 (2005).